

# Application of the Integrated Conductimetric Method to Screen Flow Systems Involving Fast Chemical Reactions

Fernando A. Iñón<sup>1</sup>, Francisco J. Andrade<sup>1</sup>, Mabel B. Tudino<sup>1\*</sup>

<sup>1</sup>Laboratorio de Análisis de Trazas. Departamento de Química Inorgánica, Analítica y Química Física/INQUIMAE. Facultad de Ciencias Exactas y Naturales. UBA. Ciudad Universitaria. (1428). Buenos Aires. Argentina

## Abstract

The integrated conductimetric method (ICM) was developed and applied to the study of physical dispersion in FI systems. This work screens ICM in a FI system in which a fast kinetics chemical reaction takes place. Acid-base neutralizations were chosen, and the influence of FIA operational variables (manifold geometry, carrier flow rate, carrier to sample concentration ratio, etc.) on conductance ( $G$ ) vs. time ( $t$ ) profiles was assessed. Experimental results show that neutralization promotes the formation of non-conductive species which lead to diminish the conductance of the system with time. ICM can be applied to monitor the formation of a product with time and to evaluate its influence on the mass transport when a single line FI manifold is used. A comparison between  $G$  vs.  $t$  profiles for systems with no chemical reaction and their analogues involving a neutralization process is given. Obtained results are fully discussed.

**Keywords:** dispersion, integrated conductimetric method, fast kinetics chemical reaction, products evolution.

## 1. Introduction

Studies on dispersion in flow injection are relevant as the analytical performance of a given method can be improved by controlling physical and chemical dispersion of the system.

Initial studies of the effects of chemical reaction on dispersion were presented by Ruzicka y Hansen [1] who defined the overall dispersion coefficient  $D_T$  as the sum of a physical ( $D_f$ ) and a chemical ( $D_q$ ) contribution:  $D_T = D_f + D_q$ .

Some reviews have given an overview on these topics [2, 3]. Andreev and Khidekel [4] developed a mathematical model considering that sample and reagents are homogeneously mixed before being injected into the flow system. Painton and Mottola [5, 6] studied the kinetics of mixing of reactants in flow conditions based on the knowledge of the classical theory of chemical kinetics. Wada et al. [7] compared signals obtained through computer simulations for systems with and without chemical reaction and concluded that the reaction kinetics can contribute significantly to signal profiles. Brooks et al. [8] studied the influence of flow rate in a FI system with chemical reaction and concluded that at low flow velocities the product formation is the paramount factor in determining the peak width and that at higher values the effect of chemical reaction is less noticeable. Reijn et al. [9] also found that, at high flow rates, the variance of a FIA curve was virtually independent of the reaction rate for a single bed string reactor manifold. Korenga and coworkers studied the effects of miniaturization of the flow injection apparatus [10, 11, 12] and the influence of chemical diffusivity on peak shapes [13].

In order to give support to the study of the dispersion process in flow systems with chemical reaction, the authors tested the integrated conductimetric method (ICM) [14] for monitoring a product formation as function of time, which is not possible through the conventional stimulus-response methodology [15].

As described before [14], ICM monitors the electrical conductance ( $G$ ) of a whole flow system as function of time by placing platinum electrodes in both ends, that is before the injection valve and after the reactor. The injection of a dielectric fluid (water) into an electrolytic carrier (e.g.,  $\text{HNO}_3$ ) produces a characteristic profile  $G$  vs.  $t$  which depends on the hydrodynamic characteristic of the FI system and it can be assigned to the mass redistribution of the injected pulse along the tube. This work is devoted to analyse the utility of ICM for studying dispersion in presence of a chemical reaction, emphasizing the influence of the kinetics of mixing of reactants. Since this influence is better noticed through the use of fast chemical reactions, acid-base neutralisations were chosen (*i.e.*,  $\text{NaOH} + \text{HCl}$ ). These neutralisations provide sharp changes in the number of charge-transport species allowing a better observation of the process.

Electrical conductance vs. time ( $G$  vs.  $t$ ) profiles were obtained for the injection of different solutions -able to react or not with the carrier- in a single line flow system. The influence of manifold geometry, carrier flow rate, carrier to sample concentration ratio and different pairs carrier-sample was assessed and it will be discussed throughout the work. Comparison with the typical FI response curves will be also provided.

\* Corresponding author.

Email: tudino@q1.fcen.uba.ar

## 2. Experimental

### 2.1. Reagents

Analytical reagent grade chemicals (HCl, NaOH, NaCl, NH<sub>4</sub>Cl, NH<sub>3</sub>; Merck, Darmstadt, Germany) and purified water (18 MΩ·cm<sup>-1</sup>) were used. Working solutions with different concentrations were prepared and employed as injected or carrier solutions.

### 2.2. Apparatus

Apparatus was shown in reference [14]. Conductimetric measurements were performed by using a digital conductimeter (Wissenschaftlich Technische Werkstätten LF 521) with a couple of Pt wires (0.03 cm diameter) located at points A-B or B (Fig. 1) in home-made flow cells. In this way it was possible to perform one-point (B) or integrated (A-B) conductimetric measurements. Fixed-point conductimetric measurements were performed with a conductimetric cell (located at point B) similar to the one described by Taylor and Nieman [16].

Signals were acquired via a data acquisition system (Keithley 1 DAS 801) and processed with a personal computer. A trigger was connected between the valve and the computer in order to start the acquisition phase when the valve is commuted.

### 2.3. Procedure

#### 2.3.1. Integrated conductimetric detection (ICD)

$G$  vs time profiles [14] for different pairs sample/carrier were obtained with the flow system shown in Figure 1. The influence of carrier flow rate ( $q$ ), loop ( $l$ ) and reactor ( $L$ ) length, tube radius ( $a$ ) and reactor geometry was assessed. As conductivity depends on the distance between points A and B, the conductivity axis ("y") was normalized for comparative purposes [14]. The obtained value,  $G^*$ , ranges from 0 to 1 and it represents the recovered fraction of the carrier conductivity after the disruption.

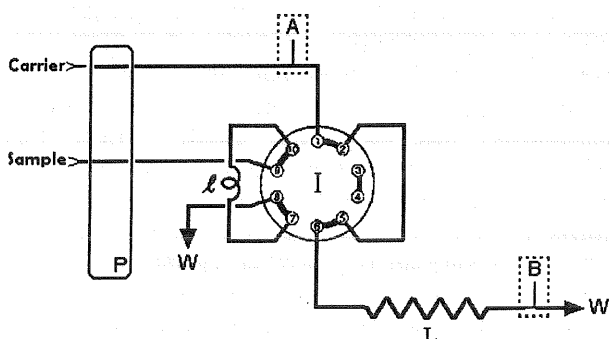


Fig. 1 Experimental set-up: P = Pump,  $l$  = loop,  $L$  = reactor,  $W$  = waste; A, B = detection points. Carrier and sample solutions were changed along the experiments.

#### 2.3.2 Single-point conductimetric detection

The experiments described in the previous section were repeated with the FI system shown in Fig. 1 locating both Pt electrodes at point B. The arrival time ( $t_a$ ) of the injected sample was obtained for all the systems under study.

## 3. Results and Discussion

Table 1 provides equivalent conductivity at infinite dilution of the ions relevant to this work as they are helpful to analyse ICM profiles.

Table 1 Equivalent conductivities ( $\lambda_0$ ) at 25°C [17].

	$\lambda_0$ (S cm <sup>2</sup> equiv <sup>-1</sup> )
H <sup>+</sup>	350
Na <sup>+</sup>	60
NH <sub>4</sub> <sup>+</sup>	73
K <sup>+</sup>	74
OH <sup>-</sup>	198
Cl <sup>-</sup>	76
NO <sub>3</sub> <sup>-</sup>	71

By using different solutions as carrier and sample, typical  $G^*$  vs.  $t$  profiles were obtained and correlated with the processes within the system. The generation and/or depletion of charged species were monitored as changes in the conductance as function of time. As the acid-base neutralisation reaction is fast, the limiting step for the reaction to proceed is the mixing of reactants. On this topic, it is expected to obtain information through ICM.

#### 3.1. Performance of the detection system

The stability of the base line was evaluated using solutions of HNO<sub>3</sub>, HCl and NaCl of the same conductivity ( $\kappa$ ). These solutions do not react between each other and were employed alternatively as sample or carrier. No significant fluctuation of the measured conductivity was observed (beyond the variation produced by the change in the distance between points A and B due to the interposition of the loop in the carrier stream [14]). Fig. 2 shows the curves obtained when NaCl solutions of different concentrations are injected into a HCl carrier. As the conductivity of the injected solutions approaches that of the carrier, the redistribution process is less noticeable. This observation is independent of the chemical identity of the electrolyte (KCl and NH<sub>4</sub>Cl were also tested).

#### 3.2. Characteristics profiles

Fig. 3 shows the ICM profiles obtained after the injection of H<sub>2</sub>O (a dielectric which do not react with the carrier), NaCl (an electrolyte which do not react with the carrier) and NaOH (an electrolyte which do react with the carrier) in a 0.2 M HCl carrier solution.

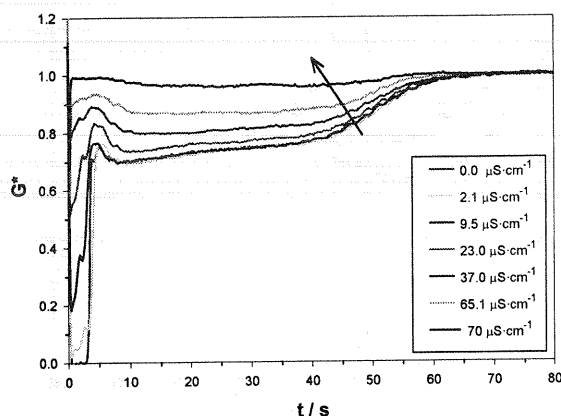


Fig. 2 Conductivity in absence of chemical reaction  $L = 100$  cm,  $l = 10$  cm,  $a = 0.025$  cm,  $q = 0.64$  cm<sup>3</sup>·min<sup>-1</sup>, carrier HCl ( $\kappa_{carrier} = 74$   $\mu\text{S}\cdot\text{cm}^{-1}$ ). NaCl samples of different conductivities ranging between 0 and 70  $\mu\text{S}\cdot\text{cm}^{-1}$  (the arrow indicates the increase in conductivity of the sample).

As it was discussed elsewhere[14,18,19], when a dielectric is injected, ICM profile is ascribed to the mass redistribution of the sample plug. Nevertheless, when an "inert" electrolyte as NaCl is injected in the carrier solution of nearly the same conductance, the ICM method is not sensitive to this process.

When a sample plug of NaOH is injected in a HCl carrier (both solutions of nearly the same conductance), the neutralisation takes place and it can be observed that the initial conductance is similar to that of the NaCl experiment. However, as time elapses, a decrease in  $G$  is noticed. This fact can be attributed to the chemical reaction that occurs inside the tube: at the contact surface between the sample plug and the carrier solution there is a depletion of species with high equivalent conductivity ( $\text{H}^+$  and  $\text{OH}^-$ ) which are replaced by others ( $\text{Cl}^-$  and  $\text{Na}^+$ ) with much lower  $\lambda_0$  than the formers (see Table 1). Similar experimental curves are obtained for other electrolytes such as KOH or NaAcO. Under the experimental boundary conditions, ICM is an useful way to follow product formation with time when the reactants present large differences on their equivalent conductivities. Small differences are not noticed.

Since the kinetics of the neutralisation reaction is fast, the rate of mixing of reactants is the limiting step and thus, whilst the contact between reactants is provided, the reaction takes place and the experimental curves reflect the degree of mixing sample/carrier.

In summary, three different responses can be observed:

- when sample and carrier have about the same conductance, the mass redistribution is not detected and the ICM profile is not affected;
- when the neutralisation reaction replaces high  $\lambda_0$  species ( $\text{H}^+$  and  $\text{OH}^-$ ) by lower ones ( $\text{Na}^+$  and  $\text{Cl}^-$ ), a decrease in  $G^*$  is observed;

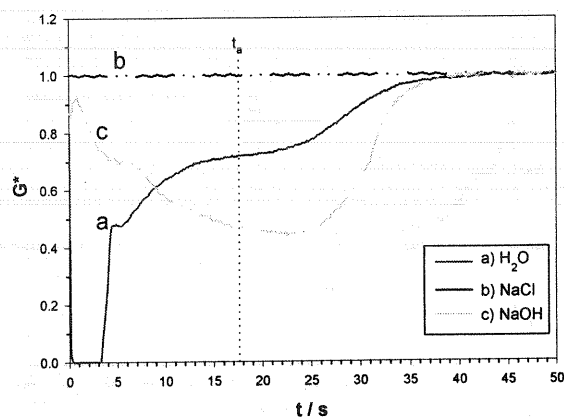


Fig. 3 Characteristic profiles.  $L = 100$  cm,  $l = 15$  cm,  $a = 0.025$  cm,  $q = 0.50$  cm<sup>3</sup>·min<sup>-1</sup>, Carrier = HCl 0.2 M, Sample: H<sub>2</sub>O, NaCl (same  $\kappa$  than carrier), NaOH (0.2 M)

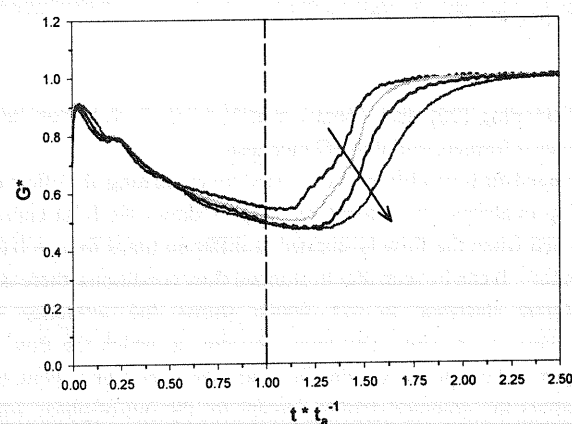


Fig. 4 ICM profiles at different  $q$  values  $L = 100$  cm,  $l = 15$  cm,  $a = 0.025$  cm, The arrow indicates an increase in  $q = 0.26, 0.42, 0.63, 1.12$  cm<sup>3</sup>·min<sup>-1</sup>; Carrier = HCl 2M, Sample= NaOH 2 M.

- when the conductance of the products is smaller than that of the carrier, an increase in  $G^*$  is observed since the mass redistribution process tends to equal  $G^*$  to that of the carrier. (see Fig. 2).

Taking into account these effects, the influence of FIA variables on the experimental profiles when NaOH is injected in a HCl carrier solution will be evaluated along the next sections.

### 3.3. Influence of some variables on ICM profile

#### 3.3.1 Flow velocity ( $q$ )

Fig. 4 shows ICM profiles at different flow rates. As it can be seen, for  $t < t_a$  there are not significant differences when the flow rate is greater than 0.6 cm<sup>3</sup>·min<sup>-1</sup>. For lower flow values, higher  $G^*$  values are obtained. This fact should be explained as follows: as  $q$  values become smaller, the flow-pattern approaches to that of

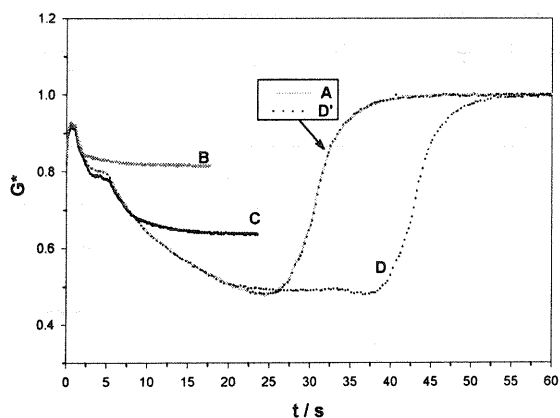


Fig. 5 Evolution of ICM profiles under stopped-flow conditions  $L = 100$  cm,  $l = 15$  cm,  $a = 0.04$  cm,  $q = 0.63$  cm<sup>3</sup>·min<sup>-1</sup>, carrier = HCl 2.0 M, sample = NaOH 2.0 M; **A** = non-stopped flow curve; **B**, **C**, **D** = stopped-flow at different times ; **D'** = curve D, but correcting the phase shift (see text).

the flow-plug [20], less contact sample/carrier is achieved, less product is formed, and thus,  $G$  increases.

Stopped-flow conditions were tested for evaluating the effect of mixing in absence of convection. Fig. 5 shows the ICM curves obtained when the flow is stopped at different times for  $q = 0.63$  cm<sup>3</sup>·min<sup>-1</sup>. It can be seen that in stopped flow conditions, there is a negligible decrease in  $G^*$  which shows the influence of convection on mixing. Moreover, the time at which the flow is stopped and the period of time in which this condition is held, do not affect the obtained profile, except for the out-of-phase with time which, once corrected (curves D y D' in Fig. 5) allows to evidence a perfect match between the ICM curves. (Fig. 4 and Fig. 5).

Experiments show that reagents are redistributed favouring their contact and thus the product formation, the product is also redistributed. As the consumption of charged-transport species promote conductivity changes, those changes in  $G$  vs.  $t$  profiles show the degree of contact sample/reagent driven by the convective-diffusive transport.

### 3.3.2 NaOH concentration

In order to study the influence of the concentrations of sample (NaOH) and carrier (HCl) on ICM profiles (Figure 6), experiments were carried out by injecting NaOH under sub-stoichiometric, stoichiometric and over-stoichiometric conditions with respect to HCl concentration. When NaOH concentration is:

- equal to that of the carrier, the conductance diminishes until the sample leaves the system.
- lower than that of the carrier,  $G^*$  decreases until the reaction is completed, then, the mass redistribution of products is observed until the sample leaves the system.
- higher than that of the carrier,  $G^*$  diminishes until  $t = t_a$ .

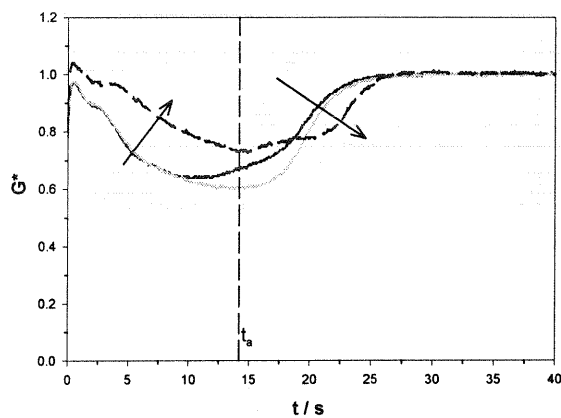


Fig. 6 Influence of NaOH concentration  $a = 0.025$  cm,  $q = 0.64$  cm<sup>3</sup>·min<sup>-1</sup>,  $L = 100$ cm,  $l = 15$ cm, HCl 0.45 M ( $\kappa = 72$   $\mu$ S·cm<sup>-1</sup>), NaOH 0.35, 0.42 y 0.84 M ( $\kappa = 57, 69$  y 134  $\mu$ S·cm<sup>-1</sup>) (The arrow indicates the increase in NaOH concentration).

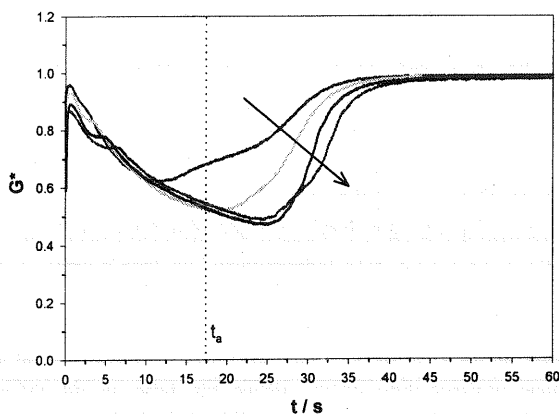


Fig. 7 Influence of loop length  $L = 100$  cm,  $a = 0.025$  cm,  $q = 0.50$  cm<sup>3</sup>·min<sup>-1</sup>, The arrow indicates the increase in  $l$ : 5, 9, 15, 21 cm; Carrier = HCl 2.0 M; Sample= NaOH 2.0 M.

An increase followed by a decrease in the measured conductance is observed at  $t$  close to  $t_a$  which is attributed to the remaining NaOH inside the sample "bolus". This fact is observed as a double peak when the detection is made at point B of Fig. 1.

### 3.3.3 Loop length (l)

Fig. 7 shows the changes in  $G^*$  when  $l$  is increased.  $G^*$  reaches its minimum value when the reaction is completed. Then, the mass redistribution of the product is observed only if the time elapsed between  $t$  at the minimum of  $G$  and  $t_a$  is long enough (see Fig. 6 for different NaOH concentrations). Since the mass redistribution process is not observed until the reaction is completed, it is clear that for a given loop length, there is a manifold length in which the mixing can be considered complete. For larger manifolds, physical dispersion is the paramount factor determining global dispersion. [19, 20].

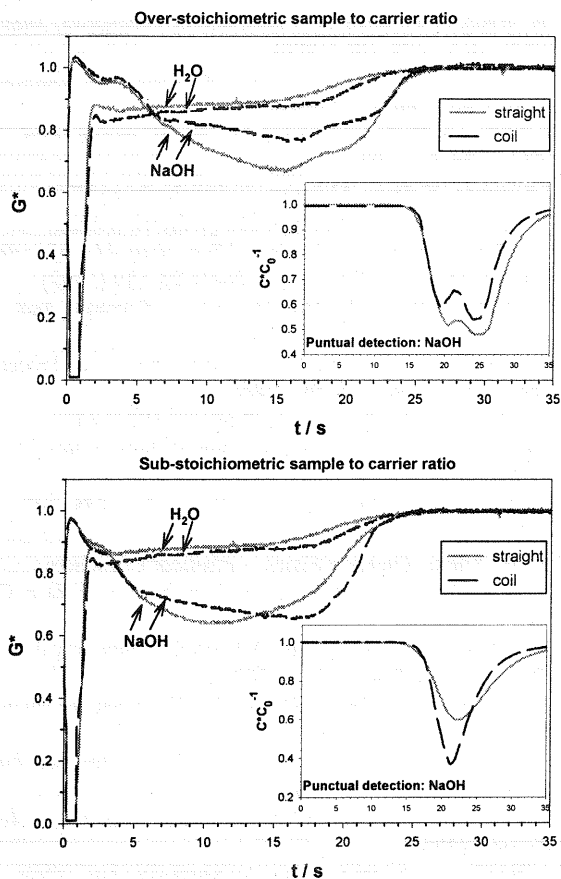


Fig. 8 Influence of manifold geometry  $L = 100$  cm,  $l = 10$  cm,  $a = 0.025$  cm,  $q = 0.64$  cm<sup>3</sup>·min<sup>-1</sup>, carrier: HCl, sample: NaOH in sub- and over-stoichiometric conditions.

### 3.3.4 Manifold geometry

Fig. 8 shows the effect of manifold geometry on the experimental curves. No differences between straight or coiled reactors are observed for short times. So, below a given manifold length, it should not be necessary to coil the tube.

In the case of sub-stoichiometric conditions, although coiled reactors reduce the amount of product, the transient signal is enhanced (in-set graph).

The case of the sample in over-stoichiometric conditions shows that coiled reactors produce a depletion of reagents within the plug boundaries (a humped peak is observed in the in-set graph), and so, less product is being formed. On the other hand, although straight reactors yield greater physical dispersion, the contact between reactants is increased, and a wider and taller peak is obtained.

### 3.4. NH<sub>3</sub> neutralization

The ICM curves obtained when a dielectric (i.e., NH<sub>3</sub>) that reacts with the carrier is injected in a single-line flow system were

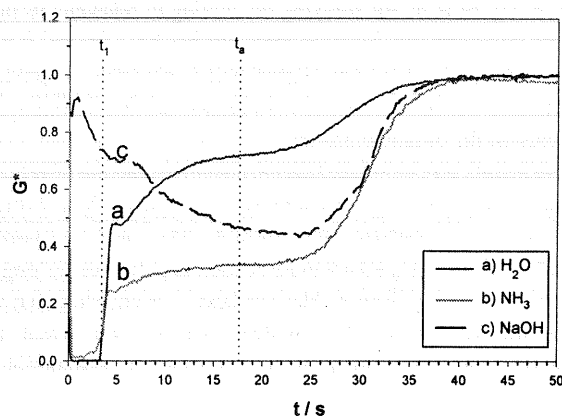


Fig. 9 Profiles for the injection of NH<sub>3</sub>, H<sub>2</sub>O and NaOH  $L = 100$  cm,  $l = 15$  cm,  $a = 0.025$  cm,  $q = 0.50$  cm<sup>3</sup>·min<sup>-1</sup>, Carrier = HCl (0.2 M), Sample = H<sub>2</sub>O, NaOH (0.2 M), NH<sub>3</sub> (0.2 M).

also tested. The global conductivity balance for this reaction is the consumption of H<sup>+</sup> and the formation of NH<sub>4</sub><sup>+</sup>, which has a conductivity 4.5 times smaller than H<sup>+</sup>.

In the case of the mass-redistribution process, the  $G^*$  vs.  $t$  curve for the injection of NH<sub>3</sub> in NaCl is the same that for the injection of H<sub>2</sub>O in HNO<sub>3</sub> or in NaCl. On the other hand, as the chemical reaction consumes H<sup>+</sup>, it produces a decrease in  $G^*$  as in the case of NaOH. Fig. 9 shows a comparison of the experimental curves obtained for H<sub>2</sub>O, NH<sub>3</sub> and NaOH injection in HCl carrier.

The profile for the injection of NH<sub>3</sub> is similar to that of H<sub>2</sub>O up to  $t = t_1$  [14], in which a partial recover of the carrier conductivity is observed. Nevertheless, the measured conductivity for NH<sub>3</sub> injection is lower. It is interesting to note that the extension of zone III (from  $t_a$  onwards), which is related with FIA peak width [19, 21], is nearly the same for both reagents, NH<sub>3</sub> and NaOH. As the concentration of NaOH is equal to that of NH<sub>3</sub>, FIA peak width has to be the same. This fact allows to perform FI titrations as described by Ruzicka and coworkers [22,23].

### 3.5. Masking the reaction

In order to analyse only the effects of the mass redistribution process on dispersion, the influence of the chemical reaction was masked. An inert acid-base electrolyte (NaCl) was added to the carrier and thus, the contribution of H<sup>+</sup> to the total system became less noticeable: the replacement of H<sup>+</sup> by NH<sub>4</sub><sup>+</sup> is not observed when NaCl is added and the response only involves the mass redistribution process. It was observed that when NaOH is injected in HCl with the addition of 10% NaCl, the decrease in conductivity due to chemical reaction is not observed and the mass distribution profile is similar to that of Fig. 2.

## 4. Conclusions

The utility of ICM for studying the mixing of reactants in flow systems involving fast chemical reactions has been shown. It was observed that ICM should be of great help to elucidate the process of transient formation and the influence of the different FI variables on the obtained profile.

Experiments give evidence that the chemical reaction affects the mass distribution of the injected pulse since it takes place through difusional contact between the reactants. The mass transport is also affected since a gradient modification is promoted as long as the product is being formed. Nevertheless, it is expected that the slower the kinetics of the involved reaction, the lesser the influence of both phenomena, which is the current assumption in FIA

### Acknowledgment

The authors thank the program for Science and Technology of the University of Buenos Aires University (UBACyT), Fundación Ciencias Exactas, and INQUIMAE for financial support.

### References

- [1] J. Ruzicka, and E. H. Hansen, *Anal. Chim. Acta*, **99**, 37 (1978).
- [2] S. D. Kolev, *Anal. Chim. Acta*, **308**, 36 (1995).
- [3] R. DeLon Hull, R. E. Malic, and J. G. Dorsey, *Anal. Chim. Acta*, **267**, 1 (1992).
- [4] V. P. Andreev, and M. I. Khidekel, *Anal. Chim. Acta*, **278**, 307 (1993).
- [5] C. C. Painton, and H. A. Mottola, *Anal. Chem.*, **53**, 1713 (1981).
- [6] C. C. Painton, and H. A. Mottola, *Anal. Chim. Acta*, **154**, 1 (1983).
- [7] H. Wada, A. Hiraoka, A. Yuchi, and G. Nakagawa, *Anal. Chim. Acta*, **179**, 181 (1986).
- [8] S. H. Brooks, D. V. Leff, M. H. Torres, and J. G. Dorsey, *Anal. Chem.*, **60**, 2737 (1988).
- [9] J. M. Reijn, W. E. van der Linden, and H. Poppe, *Anal. Chem.*, **56**, 943 (1984).
- [10] T. Korenaga, X. Zhou, M. Izawa, T. Takahashi and T. Moriwake, *Anal. Chim. Acta*, **261** (1-2), 67 (1992).
- [11] T. Korenaga and K. Stewart, *Anal. Chim. Acta*, **214**, 87 (1988)
- [12] T. Korenaga, *Anal. Chim. Acta*, **261**(1-2), 539 (1992)
- [13] L. Jinkin, L. Guojun, M. Huichang and T. Korenaga, *Anal. Chim. Acta*, **310**(2), 329 (1995)
- [14] F. J. Andrade, F. A. Iñón, M. B. Tudino, and O. E. Troccoli, *Anal. Chim. Acta*, **379**, 99 (1999).
- [15] W. E. van der Linden, in J. L. Burguera (Ed.): *Flow Injection Atomic Spectroscopy*, Marcel Dekker, New York (1989).
- [16] D. Taylor, and T. Nieman, *Anal. Chim. Acta*, **159**, 397 (1984).
- [17] P. W. Atkins, *Química Física - Physical Chemistry*, Addison-Wesley Iberoamericana, New York (1978), p. Cap 26.
- [18] F. J. Andrade, *Ph D. Thesis*, DQIAyQF, University of Buenos Aires, Buenos Aires 2001
- [19] F. A. Iñón, *Ph D. Thesis*, DQIAyQF, University of Buenos Aires, Buenos Aires 2001
- [20] J. T. Vanderslice, A. G. Rosenfeld, and G. R. Beecher, *Anal. Chim. Acta*, **179**, 119 (1986).
- [21] F.A. Iñón, F.J. Andrade and M.B. Tudino, *Anal. Chim. Acta*, in press (2002).
- [22] J. Ruzicka, E. H. Hansen, and H. Mosbaek, *Anal. Chim. Acta*, **92**, 235 (1977).
- [23] J. Ruzicka, and E. H. Hansen, *Flow Injection Analysis*, Wiley, New York (1988).

(Received October 10, 2002)

(Accepted November 27, 2002)